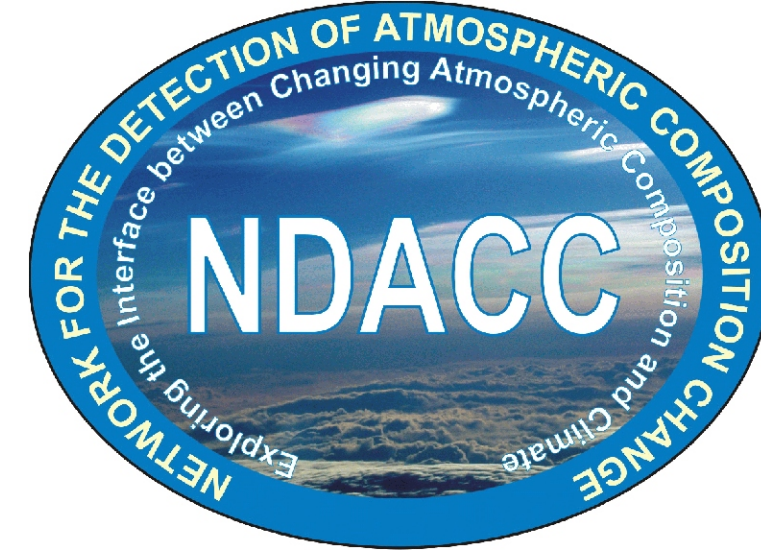


The evolution of the inorganic fluorine budget since the mid-1980s based on FTIR measurements at northern mid-latitudes

P. Duchatelet¹, W. Feng², M. Chipperfield², R. Ruhnke³, P. Bernath⁴, C. Boone⁵, K. Walker^{5,6}, P. Demoulin¹ and E. Mahieu¹



¹Institute of Astrophysics and Geophysics of the University of Liège, Belgium

²Institute for Climate and Atmospheric Science, School of Earth and Environment, University of Leeds, UK

³Institute for Meteorology and Climate Research, Karlsruhe Institute of Technology, Germany

⁴Department of Chemistry, University of York, UK

⁵Department of Chemistry, University of Waterloo, Canada

⁶Department of Physics, University of Toronto, Canada

1. Databases and methodology

In this work, we define the total inorganic (F_y^*) and total organic (CF_y) fluorine as follow:

$$F_y^* = [HF] + 2 \times [COF_2] \quad (1)$$

$$CF_y = [CFC-11] + 2 \times [CFC-12] + 3 \times [CFC-113] + 4 \times [CFC-114] + 5 \times [CFC-115] \\ + 2 \times [HCFC-22] + [HCFC-141b] + 2 \times [HCFC-142b] + 2 \times [H-1211] + 3 \times [H-1301] \quad (2)$$

where the brackets designate the total (or partial) vertical abundance of a given species, where CFC-, HCFC- and H- stand for ChloroFluoroCarbon, HydroChloroFluoroCarbon and Halon, respectively and where each fluorine species is weighted by the number of its fluorine atoms.

COCIF was not included in our inorganic inventory as its detection from ground-based FTIR measurements at Jungfraujoch is problematic, principally due to strong interferences with water vapor. Such exclusion does not constitute a critical issue since HF and COF_2 altogether represent an excellent proxy - denoted here by F_y^* - for inorganic fluorine at northern mid-latitudes (see panel #2).

All datasets involved in our fluorine inventory are presented in Table 1. According to Eq. (1), HF and COF_2 (when available) daily mean time series have been summed over the 1985–2010 time period to produce inorganic fluorine F_y^* data sets. An example of corresponding FTIR monthly mean time series is displayed in Figure 1. For both KASIMA and SLIMCAT CTMs, we have considered HF and COF_2 modeled daily values for all coincident day with FTIR observations. For satellite data, individual observations recorded in the [41–51]°N latitude belt have been selected and averaged to produce daily mean partial column time series, whose altitude ranges are provided in Table 1. No time coincident criterion with FTIR data has been applied, in order to maximize the number of data available for the trend analysis. The time periods covered by the satellite observations are also shorter, as specified in the last column of Table 1.

Data set	Description	Location	Products ^a	Covered time span for this study
FTIR	Ground-based solar IR absorption observations	Jungfraujoch station (46.5°N, 8°E, 3580m)	HF, COF_2	March 1984 - December 2010
KASIMA	3-D Chemical Transport Model	Data simulated for the Jungfraujoch	HF, COF_2	January 1985 - December 2010
SLIMCAT	3-D Chemical Transport Model	Data simulated for the Jungfraujoch	HF, COF_2	January 1985 - July 2010
HALOE v19	Satellite observations by solar occultations	[41–51]°N latitude belt	HF [15–35]	October 1991 - September 2004
ACE-FTS v3	Satellite observations by solar occultations	[41–51]°N latitude belt	HF [15–55], COF_2 [15–35]	March 2004 - September 2010

^aProvide the name of gases for which total columns are derived. For satellite data, only partial columns are available. The altitude ranges of these partial columns are specified in kilometers between the brackets, for each molecule.

Table 1 - Some characteristics of the five datasets used in our inorganic fluorine inventory.

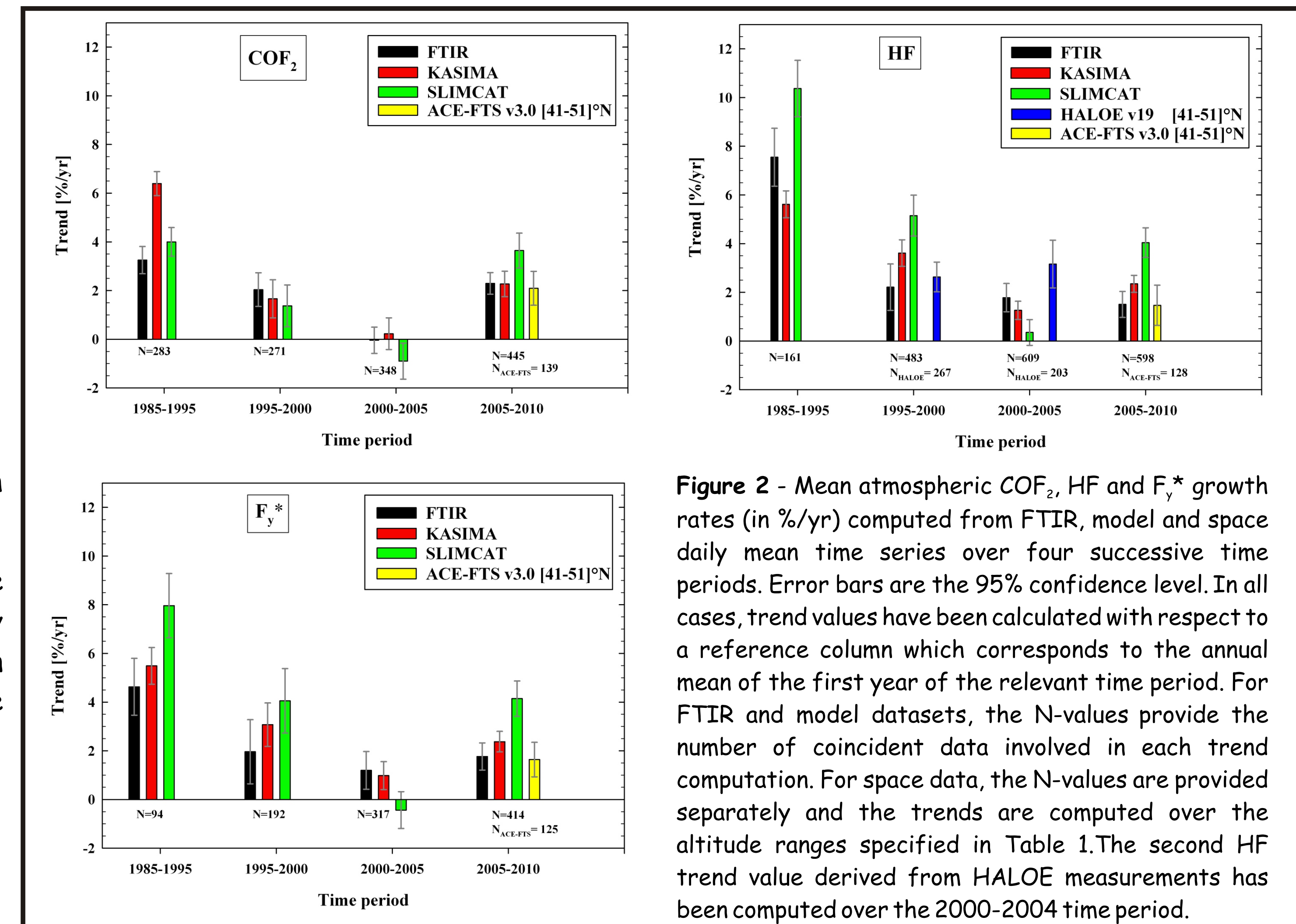


Figure 2 - Mean atmospheric COF_2 , HF and F_y^* growth rates (in %/yr) computed from FTIR, model and space daily mean time series over four successive time periods. Error bars are the 95% confidence level. In all cases, trend values have been calculated with respect to a reference column which corresponds to the annual mean of the first year of the relevant time period. For FTIR and model datasets, the N-values provide the number of coincident data involved in each trend computation. For space data, the N-values are provided separately and the trends are computed over the altitude ranges specified in Table 1. The second HF trend value derived from HALOE measurements has been computed over the 2000–2004 time period.

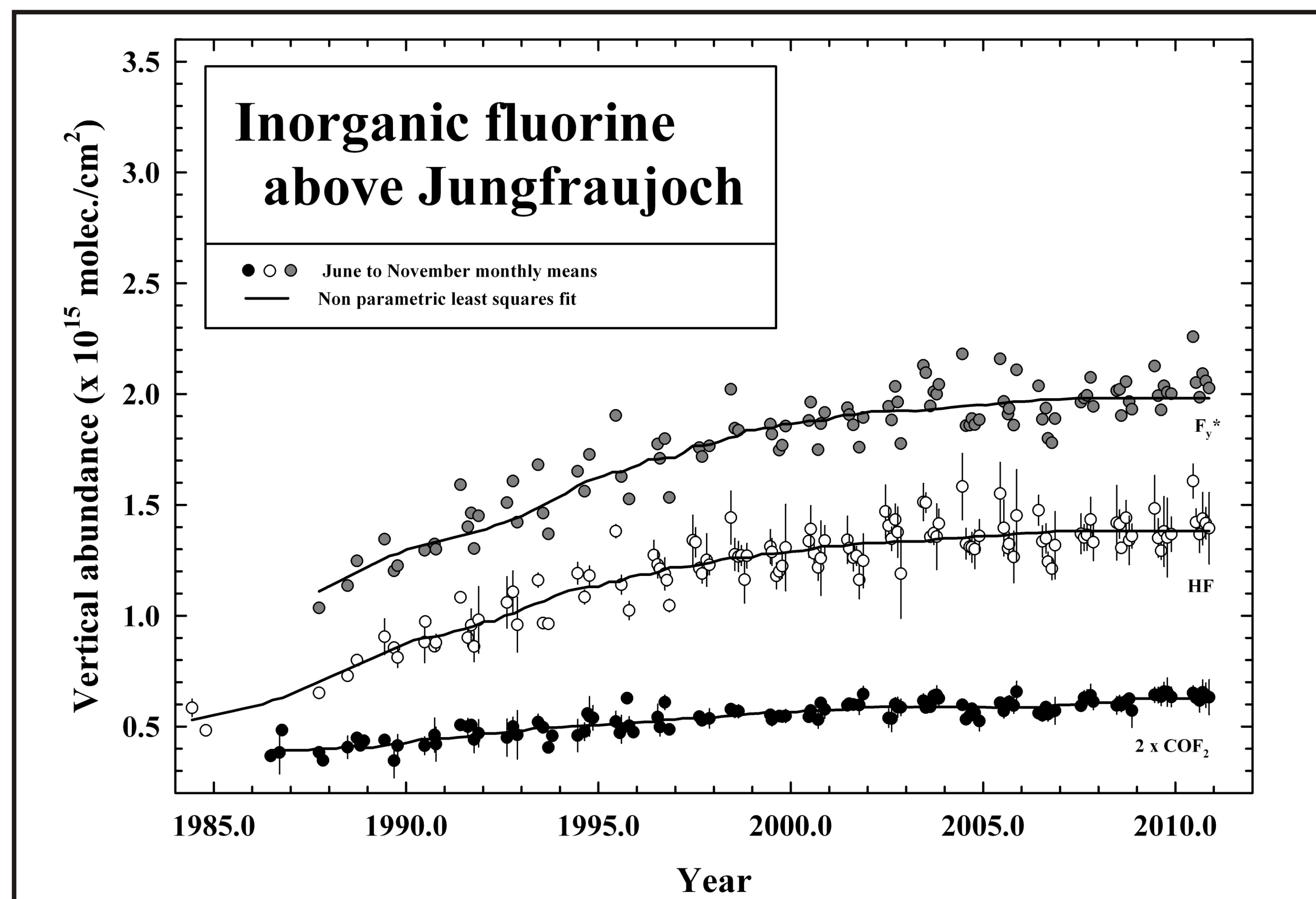


Figure 1 - Time series of monthly mean total vertical column abundances of $2 \times COF_2$ (black dots), HF (white dots) and their sum F_y^* (grey dots) derived from FTIR measurements at Jungfraujoch between 1984 and 2010. Only measurements from June to November are shown to avoid the significant variability observed during winter and spring. The black curves through each time series represent non-parametric least squares fits, in order to better appraise their temporal evolutions. For the two lower time series, error bars are 1- σ standard deviation around monthly mean values. The retrieval strategies used to derive the HF and COF_2 time series are described in Duchatelet et al. [2010] and Duchatelet et al. [2009], respectively.

2. Trend analysis

Trend values for four successive time periods (namely 1985–1995, 1995–2000, 2000–2005 and 2005–2010) have been deduced from FTIR, model and space daily mean time series (produced by following the method described in panel #1) by using a bootstrap resampling approach [Gardiner et al., 2008]. For each time period, trends expressed in relative values are plotted in Figure 2.

The FTIR trend values reproduced on the two top panels of Figure 2 indicate a significant slowing in the mean accumulation rates of both COF_2 and HF until 2005. For COF_2 , this decrease is particularly obvious during the 2000–2005 time period. Over the last five years, our FTIR data further show a significant rise in the linear trend of this gas, at a mean rate close to the value that prevailed ten years before (i.e. about 2.3 %/yr). The trend analysis of our FTIR data set further shows a stabilization in the HF growth rate during the last ten years, at about 1.6 %/yr.

We further notice that the important changes observed in the COF_2 rate of growth during the last ten years do not significantly impact the F_y^* trend, which remains quite constant since the beginning of this century at about 1.5 %/yr. That is explained by the fact that the COF_2 contribution to total inorganic fluorine is low with respect to HF. Indeed, based on our FTIR data set, we have deduced partitioning values for HF and COF_2 close to 65% and 30%, respectively, these values remaining significantly unchanged during the last twenty-five years.

It appears from bottom panel of Figure 3 that during the three first time periods under investigation, the stratospheric increase rate of the COF_2 precursors slows significantly, as a direct consequence of the Montreal Protocol. Such a behavior qualitatively explains the significant slowing observed in the rates of growth of COF_2 during the corresponding time period. Between 2005 and 2010, the A1 emission scenario predicts a stratospheric increase for COF_2 precursors that remains almost unchanged with respect to the previous time period, probably because the stabilization or the decline of the most abundant CFCs is partially compensated by the increase of substitute products such as HCFC-22. This is however inconsistent with the significant rise observed in recent COF_2 trend values reported in Figure 2. This difference could perhaps partially result from the fact that recent HCFC-22 growth is more rapid than the one assumed in the A1 emission scenario [WMO, 2010], as also highlighted when comparing A1 curves with AGAGE measurements (see the two upper curves of top panel of Figure 3). According to A1 curves, the almost unchanged growth rate in the stratospheric CF_y loading during the last ten years lets suggest a similar behavior for the total inorganic fluorine F_y and also for HF (considering the dominant contribution of this fluorine reservoir to F_y) as indeed observed from the recent FTIR and ACE-FTS trend values. Anyway, the recent COF_2 re-increase definitely needs to be understood with the help of additional numerical model simulations.

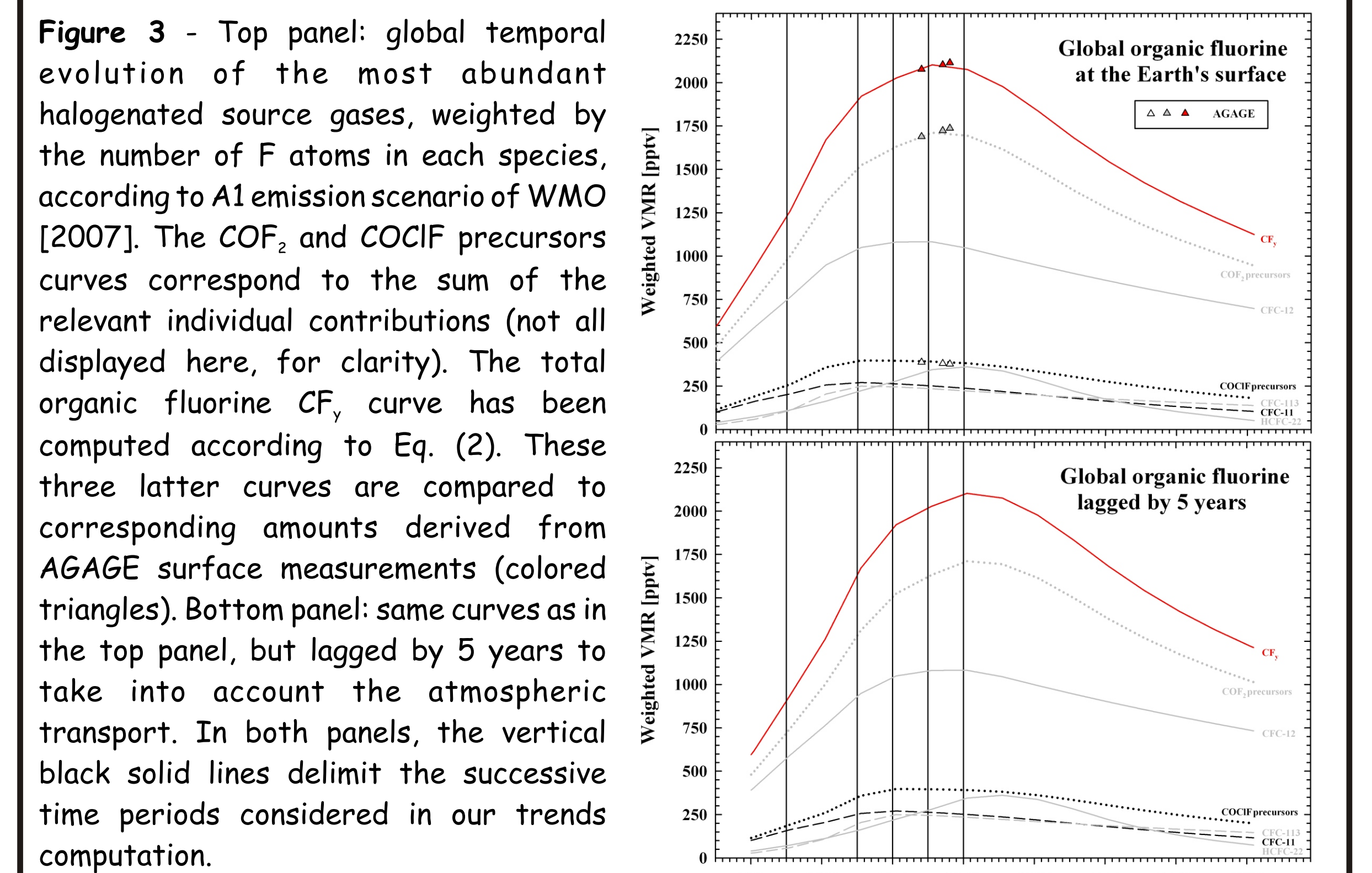


Figure 3 - Top panel: global temporal evolution of the most abundant halogenated source gases, weighted by the number of F atoms in each species, according to A1 emission scenario of WMO [2007]. The COF_2 and COCIF precursors curves correspond to the sum of the relevant individual contributions (not all displayed here, for clarity). The total organic fluorine CF_y curve has been computed according to Eq. (2). These three latter curves are compared to corresponding amounts derived from AGAGE surface measurements (colored triangles). Bottom panel: same curves as in the top panel, but lagged by 5 years to take into account the atmospheric transport. In both panels, the vertical black solid lines delimit the successive time periods considered in our trends computation.

References

- Duchatelet, P., E. Mahieu, R. Ruhnke et al., An approach to retrieve information on the carbonyl fluoride (COF_2) vertical distributions above Jungfraujoch by FTIR multi-spectrum multi-window fitting, *Atmos. Chem. Phys.*, 9, 9027–9042, 2009.
- Duchatelet P., P. Demoulin, F. Hase et al., Hydrogen fluoride total and partial column time series above the Jungfraujoch from long-term FTIR measurements: Impact of the line-shape model, characterization of the error budget and seasonal cycle, and comparison with satellite and model data, *J. Geophys. Res.*, 115, 2010.
- Gardiner, T., A. Forbes, M. De Mazière, et al., Trend analysis of greenhouse gases over Europe measured by a network of ground-based remote FTIR instruments, *Atmos. Chem. Phys.*, 8, 6719–6727, 2008.
- World Meteorological Organization, WMO Report No. 50: Scientific Assessment of Ozone Depletion: 2006, P.O. Box 2300, Geneva 2, CH 1211, Switzerland, 2007.
- World Meteorological Organization, WMO Report No. 52: Scientific Assessment of Ozone Depletion: 2010, P.O. Box 2300, Geneva 2, CH 1211, Switzerland, 2010.

Acknowledgements - We would like to thank the International Foundation High Altitude Research Stations Jungfraujoch and Gornegrat (HFSJG, Bern) and the University of Liège for supporting the facilities needed to perform the observations and their analyses. University of Liège work is supported primarily by the Belgian Federal Science Policy Office (PRODEX projects ACE and SECPEA). Additional support by the European Union GEOmon project (FP6-2006-IP-C036677) is further acknowledged. The Atmospheric Chemistry Experiment (ACE), also known as SCISAT, is a Canadian-led mission mainly supported by the Canadian Space Agency and the Natural Sciences and Engineering Research Council of Canada.